TNO's RESEARCH ON CERAMIC BASED ARMOR

Erik Carton, Geert Roebroeks, Jaap Weerheijm, André Diederen and Manfred Kwint
Group Explosions, Ballistics and Protection, TNO
P.O. Box 45, Rijswijk, The Netherlands

ABSTRACT

Several specially designed experimental techniques including an alternative test method have been developed for the evaluation of ceramic based armor. Armor grade ceramics and a range of combined materials have been tested using 7.62 AP rounds. Using the energy method [12] the dwell-time and total energy absorbed from the AP core were determined. In additional tests time-resolved fracturing of the ceramic tile (fragments) was recorded using high-speed video at one million frames per second. Also the particle size distribution of the fragments were measured in order to determine the total fracture surface area. The information provided by the results of all tests has resulted in an energy-based engineering model that allows calculation of the dwell-time, erosion and residual velocity of an AP-core. The model predicts the mass and velocity of residual AP cores rather well assuming a failure period during which the intact ceramic material transfers into a massively broken medium. The model does not require detailed mechanical properties of the ceramic materials. This reflects the difficulty within the ceramic armor research community to find a relation between mechanical properties and ballistic efficiency of armor ceramics. The developed engineering model creates a renewed understanding of the relevant phenomena, that could explain the ballistic efficiency of ceramic armor.

INTRODUCTION

Over the last years TNO's Laboratory for Ballistic Research has focused its R&D on the subject of armor ceramics, as a component of an armor system, as well as on ceramic based armor; a combination of ceramic and other materials together forming an armor system. The optimization of ceramic based armor systems is targeted by the armor community to obtain more weight efficient protection. However, armor ceramics are still not very well understood, hence there may still be a lot to gain if one can determine the main mechanisms that occur during the short interaction time between a high speed projectile and a ceramic-based armor. TNO's research has been limited to 7.62 AP rounds and therefore is mainly focused on body-armor applications, however the scope will be expanded to vehicle armor in the coming years.

Generally speaking ceramics are an effective class of armor materials as they can both erode a hard projectile (core), hence change the nose shape and reduce its mass, and project the impact forces over an area much wider than the projectile diameter. The latter will reduce stress by spreading forces exerted on the backing material, preventing its local failure thereby allowing a large volume of backing material to be involved in the projectile-target interaction.

Over the years relationships between the mechanical properties and the ballistic efficiency of armor grade ceramics have been searched for. The unique combination of mechanical properties of ceramics like high hardness, compressive strength, stiffness and relative low density are frequently mentioned to rationalize the use of ceramics in armor. However, even after decades of use the relation between mechanical properties and ballistic (protection) efficiency is not fully understood. This may be explained by also considering some other relevant mechanical properties of ceramic materials like their modest tensile strength and brittle fracture behavior. This combination of mechanical properties results in early failure and negligible energy dissipation by fracturing of ceramic materials. It is the main reason ceramics

are not used stand-alone in armor applications. Ceramics generally are supported by a backing material that is ductile and capable to absorb (residual kinetic) energy. Often metal plates or polymer fiber materials (like fabrics and composite) are used as backing material in armor systems. Hence, armor ceramics are often tested in combination with a backing material that influences the projectile-target interaction. This influence complicates the search for a unique relation between a mechanical property of the ceramic and its ballistic efficiency [1]. To complicate things further, the projectile-target interaction not only depends on intrinsic material properties of the ceramic and its backing material. Many researchers have shown that extrinsic properties, like tile dimensions, pre-stressing and confinement also have a large influence on the ballistic behavior of a ceramic-based armor system [2-5].

Figure 1 shows a schematic representation of the impact of a core of a bullet with a (bare) ceramic tile. The ceramic has high enough compressive strength to initially withstand the dynamic loading by the impacting projectile (a high strength core with conical or ogive nose shape). Hence, the first interaction phase is dwell; the interface velocity between projectile and ceramic is zero (U=0). The tail of the projectile still has the impact velocity (V), thus the length of the projectile will reduce with a velocity V-U=V. As an AP core consists of a brittle material, the failure strain is very low resulting in erosion rather than deformation of the core material. In the second image of figure 1, the eroded fragments/particles of the projectile nose can be seen to spray from the high pressure impact area below the projectile. The ceramic tile itself does not yield, and only responses by bending generating a linear strain distribution over the tile thickness inducing a compressive stress at the strike-face and a tensile stress at the rear of the tile. During the dwell phase the ceramic suffers from impact damage and/or erosion on the strike-face by the radial movement of the eroding projectile, as well as internal failure by comminution, micro- and macro-cracks. The internal damage of the ceramic tile is shown in yellow in figure 1. At a certain moment the internal damage has propagated throughout the tile thickness. This allows a localized flow of fragments and formation of a conical plug. From this moment on, the ceramic can flow axially reducing the dynamic loading (as U>0) finally eliminating the erosion of the projectile when $U=V_r$, with V_r the residual velocity of the projectile. This transition in penetration velocity (from zero to $U=V_r$) marks the end of the dwell phase ($t_{Dwell,end}$). The axial flow of fragments can be seen at the rear of the tile as this initiates an out-of-plane movement resulting in a fragment cloud that is pushed out by the residual projectile (with mass m_r and velocity V_r).

Although it has not been possible to conclusively determine a relation between mechanical properties and ballistic efficiency for ceramics, one material requirement has been identified to play an important role in the ballistic efficiency of armor ceramics: hardness or compressive strength. In order to function well, the hardness should be above a minimal value which depends on the strength and velocity of the projectile to be stopped. The relevant projectile part is normally the core of an armor piercing munition type. Jacket and filler materials of bullets are relatively soft/weak materials and are easily stripped from the core in an early stage of the interaction. Their fragments and particles mainly flow away radially over the strike-face of the ceramic armor, leaving only the core to interact with the armor. Core materials are, with increasing hardness: mild steel, tungsten heavy alloy (WHA), hardened steel and cemented carbide (WC/Co). In order to initiate a dwell-phase upon impact on its strike-face the ceramic should have a minimal compressive strength (R_t) which is related to the hardness of the ceramic (a first approximation of this compression strength is $R_t=H_v/2$) [6]. The minimal strength requirement can be rationalized using the Tate-relation (or modified Bernouilli equation) [7]:

$$\tfrac{1}{2}\rho_p (V-U)^2 + Y_p = \tfrac{1}{2}\rho_t U^2 + R_t \qquad (1)$$

In this relation R_t represents the effective compressive strength of the ceramic target and Y_p is the strength of the projectile (core) material. V is the velocity of the tail of the projectile, while U is the velocity of its front (nose), hence U is equal to the velocity of the interface.

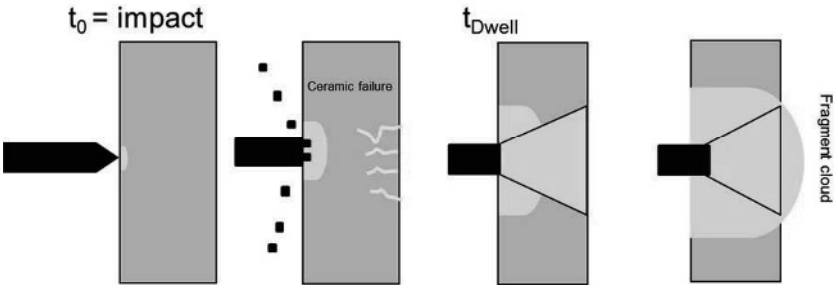

Figure 1. Schematic representation of the projectile-target interaction of a ceramic tile

During the dwell phase the nose of the projectile is stopped on the strike-face (hence U=0) and its dynamic loading is defined by the interface stress:

$$P = \tfrac{1}{2}\rho_p V^2 + Y_p \qquad (2)$$

If the ceramic compressive strength is high enough (R_t>P) it can withstand this dynamic loading of the impacting projectile (at least temporary). As the core of the projectile has (by far) the highest strength of its components, Y_p is only determined by the strength of the core of a bullet. A hardened steel projectile with a strength of Y=2 GPa impacting a ceramic at 1000 m/s will exert a dynamic pressure of about 6 GPa during the dwell phase (U=0). This means that a ceramic tile able to withstand this pressure should have a compressive strength R_t > 6 GPa. In order to induce a dwell-phase for a similar impact of a cemented carbide (ρ= 15.000 kg/m^3) the ceramic should have a compressive strength of at least 10 GPa.

Ductility parameter

Horii and Nemat-Nasser [20] describe a unit-less ductility parameter of a material surrounding a flaw with half-size c:

$$\Delta = K_{IC}/\tau(\pi c)^{1/2} \qquad (3)$$

Where τ is the shear strength and K_{IC} the fracture toughness of the material. The importance of ductility (or the inverse of brittleness) to ballistic performance was outlined by LaSalvia et al. [21, 22] using this ductility parameter Δ.

D-value

The D-value is a figure-of-merit for the ballistic energy absorption rate ability for ceramics. It is derived from an energy ratio during a static indentation process (e.g. hardness measurement) [11]. The indentation of a ceramic involves two aspects; inelastic deformation, resulting in a measurable residual indent, and fracture resulting in a number of cracks surrounding the residual indent. The energy dissipated in an inelastic zone with (residual indent) size a is approximately Ya^3, with Y the yield-stress (strength) of the material. Normally Y is proportional with hardness (H) [6], hence the inelastic deformation energy is on the order of Ha^3.

The specific fracture energy involved will be proportional to Ga^2 (assuming that the residual indent size a and the crack length are proportional). Fracture energy (G) is related to fracture toughness (K) and Young's modulus (E); $G=K^2/E$.

The ratio between inelastic deformation energy and fracture energy is used to express the brittleness of a material: $Ha^3/Ga^2 = HE/K^2 * a = B * a$
which results in a brittleness factor B that is well known in the theory of fracture mechanics of brittle materials. For application in the dynamic world of ballistics the equation has been adjusted by including the sound velocity c of the ceramic material [14]:

$$D = \frac{0.36(H_V Ec)}{K_{IC}^2} = SBc \qquad (4)$$

This D-criterion depends on the Vickers hardness (H_V), elastic modulus (E), sonic velocity (c), fracture toughness (K_{IC}) and a parameter, called structural parameter "S", which depends on the ratio between the corresponding velocity of fracture and the sonic velocity. Fracture toughness is the only parameter with a square relation to the D-value. This makes this parameter dominant in the relation. Surprisingly, this parameter is in the denominator indicating that a low toughness generates high D-values. This indicates a conflicting requirement for an armor ceramic; the efficiency to stop a bullet increases with D, hence a low toughness (K_{IC}) is better, while for stopping multi-hit threats damage in the tile should be minimal requiring a high material toughness (high K_{IC}).

D-values (in 10^{12}/s) of armor ceramics range for Alumina between 1 and 3, for SiC between 3 and 5 and for B_4C between 5 and 8. This is also the ranking in ballistic efficiency as experienced in the field. However, if one compares the D-value within a single type of ceramic (like different alumina materials), then a higher D-value does not result in a higher ballistic efficiency. Hence, also no unique relation between the ballistic efficiency and such figure-of-merit has been identified so far. This leaves us with a rather unsatisfactory conclusion that a relation between the two does not seem to exist, as has been confirmed by many other researchers [15-17].

BALLISTIC TEST METHOD

The ballistic test method performed by TNO (the energy-method) has been presented at the 38th ICACC-meeting in 2014 [12]. Referring to the article in the proceedings of this meeting, only a very brief explanation is provided here. The energy-method is based on measurement of (kinetic) energy of the core of a projectile before and after interaction with the target. This requires the mass and velocity of the core before and after its interaction to be known. The velocities are generally measured in a ballistic range, while the residual core mass is measured after its recovery using a soft catching system. The difference in kinetic energy provides the energy loss of the AP-core. This energy-loss divided by the areal density (kg/m^2) of the target provides a value for the ballistic efficiency (in J m^2/kg) of that target for that threat. Additionally, from the mass-loss of the core an estimated dwell-time (t_{Dwell}) can be obtained after calculation of its reduction in length (ΔL) due to mass erosion. The estimated dwell time can be calculated by dividing the lost core length (ΔL) by the impact velocity (V): $t_{Dwell} = \Delta L/V$. In this test method ceramic tiles can be tested both as bare tiles and with a finite backing material. The latter assures that the tiles behave as in realistic armor systems, opposite to the depth of penetration (DoP) test method in which tiles are over-supported. Also the variation in test results between shots is rather low (about 10%) requiring less tests, thus less test material needed to get reliable results. Normally a constant threat (AP-bullet and impact velocity) and only 3 samples per target

configuration are needed in a test series. Average values are calculated for both the ballistic efficiency and estimated dwell time of each sample configuration.

Graded ceramics

At the start of the TNO research effort on ceramic-based armor it was suggested that the lack of a clear relation between mechanical properties and ballistic efficiency was due to the fact that armor ceramics are homogeneous materials, while their loading is quite different at both sides of a tile; the strike-face experiences a compressive stress as it is highly loaded both dynamically and by (local) bending, while the rear of a tile experiences a tensile type of loading as a result of local bending of the tile. The strike-face needs a very high compressive strength and a low toughness (according to the D-value), while the rear of a tile needs high tensile strength, and a high toughness to avoid early failure. A homogeneous material cannot be optimized as it cannot meet these conflicting requirements. If one increases the toughness this will help to delay failure (radial cracks) at the rear to occur, but reduces the effectivity of the strike-face (lower D-value). And if the hardness in increased this will improve the effectiveness of the strike-face, but lowers the toughness and tensile strength, thereby weakening the rear of the tile which promotes the onset of radial cracking.

In order to escape from this dilemma TNO had graded ceramics manufactured at Leuven University, Belgium. Such samples have different microstructure and composition at opposite tile surfaces (strike-face and rear) and a stepped transition in between. Manufacturing of graded samples by sintering is not an easy task as each composition has its own optimal sintering condition (temperature, time and pressure) and differences in thermal expansion cause high residual stress between components due to thermal shrinkage upon cooling down to room temperature. These difficulties greatly limit the choice in ceramics that can be combined into a (step) graded sample by sintering.

At first, a survey was performed on the options of ceramic compositions that can be densified and bonded using one set of sintering conditions, while creating a large difference in fracture toughness (K_{IC}) on both sides. In order to perform useful ballistic tests the size of the samples should be large enough. As we have focused on body armor the ballistic tests are performed using 7.62 AP rounds, these require a minimal tile size of 50 mm and a minimal thickness of 5 mm [12]. After a few sintering tests on a smaller scale it proved to be possible to manufacture step graded ceramic samples composed of pure Alumina (SM8) and a Alumina-Zirconia mixture with 40 mass-percent Zirconia (Al_2O_3-40% ZrO_2, or A40Z). The outer layers had 3 mm thickness and were bonded by a 1 mm thick interlayer of Al_2O_3-20% ZrO_2. Also homogeneous samples of pure Alumina and the Al_2O_3-40% ZrO_2 (A40Z) mixture have been made. All samples that were ballistically tested were disk shaped with a diameter of 56 mm and a thickness of 7 mm. Also a commercially available armor grade Alumina (Corbit 98, Bitossi) was ballistically tested with the same tile dimensions.

Due to a small particle size of the starting materials and the short spark plasma-sintering (SPS) duration, the microstructure remained submicron-sized. This generated a high hardness, while the Zirconia addition increased the toughness (measured using indent crack length) considerably. Part of the difference in toughness of the step-graded samples was caused by the residual stress inside the sample increasing the toughness on the Zirconia rich size and reducing it at the pure Alumina side. This was concluded by comparison of these properties between monolithic (homogeneous) and step-graded samples, see table 1. Several disks of each composition have been manufactured and as these have optimized mechanical properties (high hardness combined with a large difference in toughness on both disk sides) the hypothesis of optimization of ceramics for ballistic protection purposes could be checked. The largest difference was expected between shots with the step-graded ceramics using the Alumina side as

strike-face (FGC-A) and those in which the Zirconia rich (FGC-Z) side was used as strike-face. The results of the monolithic samples were expected to lay in between these two extremes of step-graded ceramics.

The energy method was performed using 7.62 CBC bullets as these showed a small variation in impact location. This allows the samples to be hit close to the tile center and hence prevent edge effects as much as possible. In figure 2 the energy loss of the ogive nosed hardened steel core of this bullet is plot for the 7 mm thick ceramic disks.

Surprisingly, the monolithic SPS samples performed just as well as the step-graded samples. Even the two step-graded configurations with Alumina (FGC-A) or the A40Z (FGC-Z) as strike-face did not show any difference in performance. Also the dwell time of all the SPS samples proofed to be identical: 13 µs. Hence, the SPS samples did not show significant differences in ballistic performance.

Table 1. Properties of the monolithic and step-graded ceramic samples made by SPS

Type	Material	E [GPa]	ρ [kg/m^3]	Hv [GPa]	Kic [MPa √m]
Monolithic	Al2O3	390	3980	21	2,7
	A40Z	300	4800	18,2	4,1
Step graded	A/A20Z/A40Z	390	4400	20,8	1,0
	A40Z/A20Z/A	300	4400	17,8	5,6

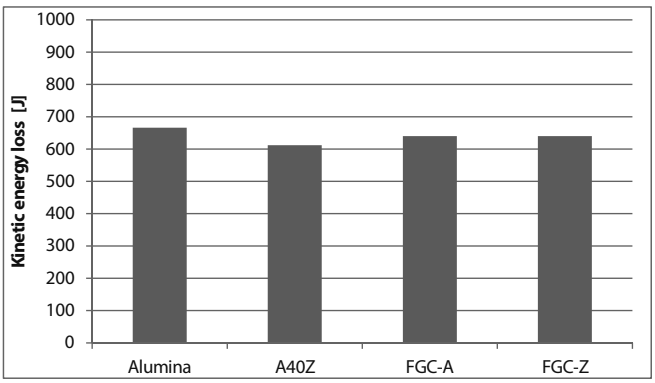

Figure 2. Energy loss of 7.62 CBC at 830 m/s on 7 mm thick targets, FGC means step-graded ceramic with –A the alumina as strike-face, and –Z the A40Z-side used as strike face.

Apparently, the differences in mechanical properties between (and inside) these samples did not lead to significant changes in ballistic efficiency of these materials. Also a number of commercially available alumina tiles of 7 mm thickness were tested as disk of Ø 56 mm (Corbit 98 with a Vickers hardness of 15 GPa). The average energy loss and estimated dwell time were

704 J and 14 µs, respectively. Both are slightly higher than obtained with the SPS samples of considerable higher hardness.

These experimental results on step-graded ceramics conflict with the hypothesis that optimal armor ceramics need different material properties for the two tile sides. Therefore this hypothesis is rejected. It once more shows that a relation between (statically measured) mechanical properties and ballistic efficiency does not seem to exist.

Adhesively bonded samples

The TNO R&D effort included investigation of the effect of tile thickness and that of backing layers. Also layered and biceramic samples have been manufactured by adhesive bonding using epoxy adhesive. Figure 3 shows the ballistic efficiency of Corbit 98 alumina tiles to increase with thickness. Due to the finite kinetic energy of the core of the bullet (7.62 APM2 at 830 m/s) above a certain tile thickness all of the energy is consumed in the interaction which limits the test set-up. This limitation is shown by the black line in figure 3 which is defined by the kinetic energy of the core ($\frac{1}{2}m_cV^2$) divided by the areal density of the tile. For the testing of thicker tiles one needs to increase the kinetic energy of the core (increase core mass and/or impact velocity).

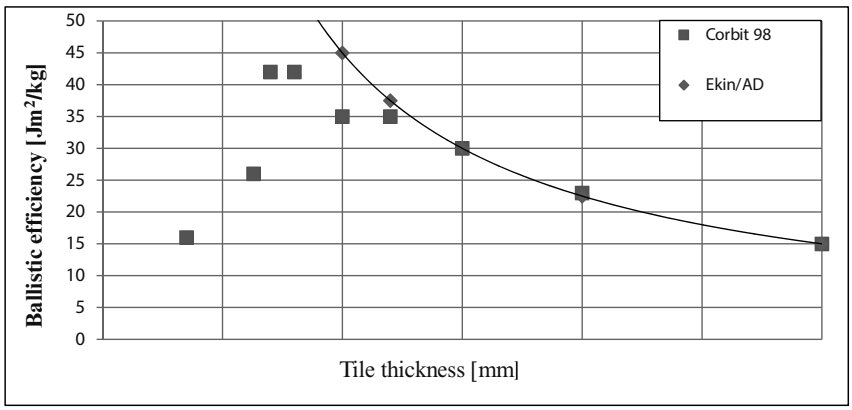

Figure 3. Ballistic efficiency versus tile thickness for Alumina (Corbit 98) against 7.62 APM2 at 830 m/s.

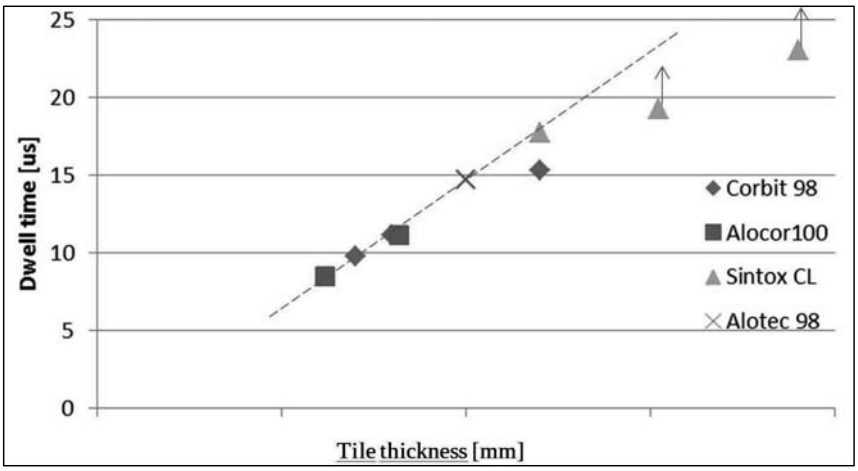

Figure 4. Dwell time versus tile thickness for bare Alumina against 7.62 APM2 at 830 m/s

In figure 4 a linear relation between estimated dwell time and (bare) tile thickness is obtained for several alumina types. Although only alumina types were used, there are quite large differences in mechanical properties between them. The hardness ranges from 12 GPa for Sintox CL to 23 GPa for Alocor100. The latter combines a SiC-like hardness with a spectacular high toughness of 6,7 MPa $m^{½}$. Nonetheless, both Sintox CL and Alocor100 nicely fit on the line between all other alumina types tested at various tile thicknesses. This is another indication that the mechanical properties of armor ceramic play a minor role in the interaction with a high speed projectile as long as its hardness (compressive strength) is higher than that of the projectile (core). The estimated dwell times of the thicker tiles lay somewhat below the line, but this is probably due to the fact that the deceleration of the core has not been taken into account. This is a neglectable effect for thin tiles, i.e. short dwell times, but should be compensated for at longer dwell times. Therefore, the estimated dwell time as obtained simply by $\Delta L/V$ provides an underestimated value, especially for thicker tiles.

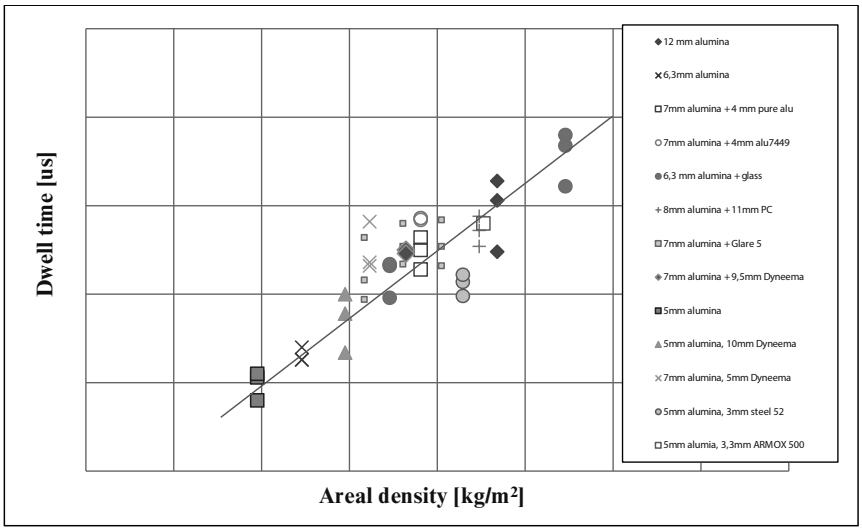

Figure 5. Dwell time versus areal density for bare alumina tiles and alumina samples with various adhesively bonded backing materials against 7.62 APM2 at 830 m/s

In figure 5 the dwell time versus areal density (tile thickness times density for bare tiles) of several Alumina samples with and without a backing material is shown. Although the backing materials have been varied widely (from glass or steel to Dyneema, UHMWPE, and polycarbonate, PC) again a linear response with areal density of the material combination is obtained. This line represents the same relation as was found for bare tiles, in figure 4. Quite spectacular differences in strength of backing materials have been used in the test series: 7 mm alumina with a very soft pure aluminum, a very strong aluminum alloy (AA 7449) and a Glare-type (a fiber metal laminate), or 5 mm alumina with a construction steel and an Armox500 armor steel as backing layer. However, all results come close to the same line as was obtained using bare ceramic tiles. So, as far as the duration of the dwell phase is concerned, not only do the mechanical properties of the ceramic not play a role (as seen earlier), but also those of the backing layer are not important. Apparently, the dwell time of a ceramic-based armor is mainly controlled by inertia (areal density) of the system.

In figures 4 and 5 the fit line does not go through the origin of the plots. The dwell time is zero at some offset in areal density or tile thickness. This means that the dwell time of very thin ceramic targets is minimal and explains the steep decrease in ballistic efficiency of alumina at small tile thicknesses, as was obtained in figure 3.

Also other ceramic materials with a hardness considerably above that of hardened steel cores (Vickers hardness of about 8 GPa) have been tested using the energy-method. Several tile thicknesses have been used on SiC, Si_3N_4 and ZrO_2. SiC is also an abundantly used armor ceramic due to its higher hardness combined with a lower density (of about 3200 kg/m^3) compared to alumina. Silicon nitride (Si_3N_4, N3000 obtained from H.C. Starck) has a similar density as SiC but is much tougher (K_{IC} = 6,5 MPa m^{½}) compared to armor grade SiC and alumina. Its Vickers hardness is about 14 GPa, which is comparable to armor grade alumina. Zirconia is the toughest ceramic (about 7 MPa m^{½}), but this is compensated by a rather high density (about 6000 kg/m^3). Its hardness (13 GPa) is comparable to that of (normal) alumina.

These ceramic tiles have both been tested as monolithic tiles and as biceramic tiles using a thin epoxy adhesive for bonding both similar and dissimilar tiles. Figure 6 shows a similar trend in dwell time versus areal density for a specific ceramic as obtained with alumina. Also the off-set in areal density for zero dwell time reappears.

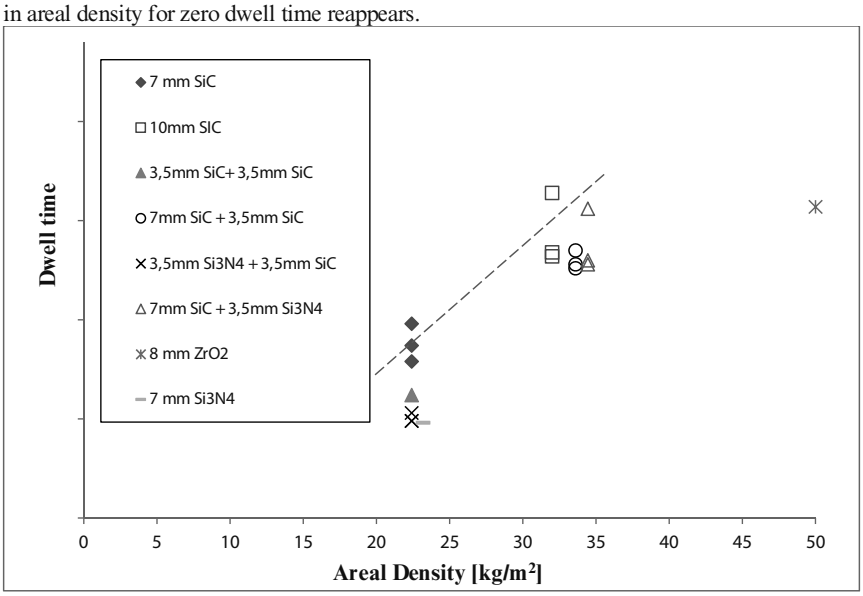

Figure 6. Dwell time versus areal density for SiC, Si_3N_4 tiles and ZrO_2 including biceramic tiles against 7.62 APM2 at 830 m/s

However, also differences are apparent; although the Si_3N_4 tiles have a similar density, hence inertia as SiC their dwell time is much lower. And the ZrO_2 tile has a similar dwell time as the 10 mm thick SiC tiles, but at a much larger areal density. This proves that areal density does not tell the full story.

From the adhesively bonded samples we learn that a single monolithic tile of a material performs better than a laminate of two thinner tiles. The dissimilar or biceramic samples enables once again to make use of a hard and brittle material (SiC) on one side and a tough, strong material at the opposite side (comparable to the step-graded SPS samples). However, also in this case did the biceramic samples perform equal or even worse compared to the monolithic samples.

ADDITIONAL EXPERIMENTS

In addition to the energy-method also completely different experiments have been performed in order to understand the projectile-target interaction of ceramic tiles. Experiments have been performed with bare tiles inside a closed steel box which enabled us to recover all fragments of the tile and determine its size distribution [13]. Also the size distribution of the aerosol fraction (formed by the finest particles) has been measured using special equipment that can measure particle sizes down to the nanometer range. A surprising large amount of nano-sized ceramic and metal particles were shown to be generated by the impact of 7.62 AP and Ball

projectiles [13]. But the calculated total new surface area of all fragments and particles together did not represent a large amount of dissipated energy [13].

Additional experiments have been performed using a high speed video camera (Shimadzu HPV-2) with a time-resolution of 1 million frames per second and 100 images per film. This provides a useful time and special resolution in order to follow damage progression inside transparent and translucent ceramic targets. Two experiments using high speed imaging are described here.

Crack shadowgraphy

From the three most used armor ceramics (alumina, SiC and B_4C) only alumina is translucent. Although not transparent multi-crystalline alumina can transmit light by scattering. The transmittance of light is greatly hindered by the presence of cracks in the material, hence the transition from an intact to a damaged state can very well be observed using shadowgraphy. Just as in the energy-method bare Alumina tiles (100x100 mm) of various thicknesses were shot normal using 7.62 mm AP-munition. The strike-face was illuminated using flash-lights, while the side and rear of the tile were observed by the high speed camera (the latter using a mirror). The incoming projectile could be seen at the rear of the tile by its shadow. Since the frame rate was set to 1 Mfps, the occurrence, order and progression of fast running cracks inside the sample could be recorded. Figure 7 shows a sequence of images of the impact of an 7.62 APM2 round (at 830 m/s) on a 7 mm thick bare alumina tile. The first image shows the moment of impact, while the middle image shows radial cracks and an expanding darkened middle region. The final image (right) shows the full size of the darkened region. It is assumed that the darkening effect is a result of internal damage (comminution and cone cracking). Radial cracks are the first to occur (as thin straight lines) while the darkened region grows in diameter. In figure 8 the radial cracks and expansion of the darkened region is shown at different times after impact (t=0). This expansion process stops suddenly. This moment is compared for several tile thicknesses and two armor grade alumina types in figure 8 (right).

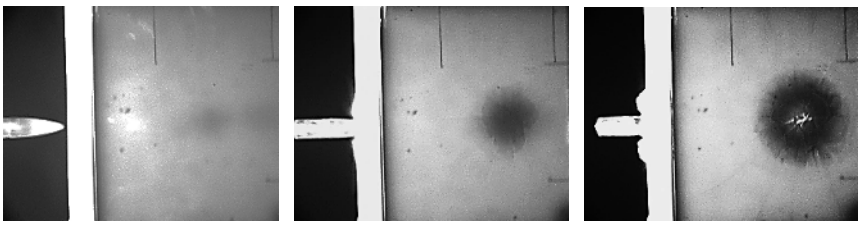

Figure 7. Side (left in images) and rear view of an alumina tile impacted by a 7.62 APM2.

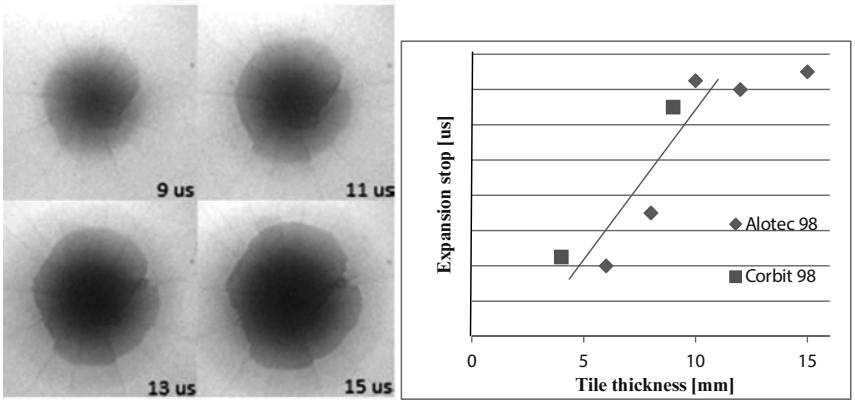

Figure 8. Left, shadowgraphs at 4 times showing radial cracks and expansion of a darkened region in a 10 mm thick Alumina tile impacted by a 7.62 APM2 round at 830 m/s. Right: Moment of expansion stop of the darkened region as function of tile thickness.

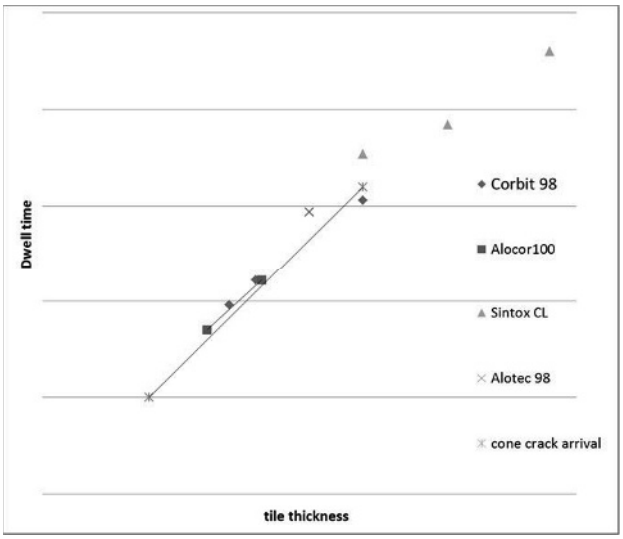

Figure 9. Dwell time (energy method) and moment of expansion stop (crack shadowgraphy) measured for Alumina tiles of various thickness and types impacted by a 7.62 APM2 round.

Again a linear relationship between this time and tile thickness is obtained. In Figure 9 the dwell time versus tile thickness of Figure 4 is plot again together with the times at which the expansion of the darkened region stopped. In the energy method the residual mass and impact velocity of the core have been used, while for the shadowgraphy tests optical images of damage evolution in the ceramic tiles are used. Figure 9 shows that these very different measuring techniques provide

the same data. The fact that the expansion of the damage stops at the same moment the dwell phase ends is in line with the view of the projectile-target interaction as shown in figure 1. From this moment on the residual projectile pushes the ceramic fragments out in a conical volume in front of it (out-of-plane deformation) and eventually a fragment cloud is formed.

Dynamic fracture visualization

Another method to visualize damage evolution in targets is to use transparent material and look inside the impacted tile from aside (side view). Squared Spinel tiles (45x45 mm) with a thickness of 7 mm have been used. In addition a single shot using a tile size of 90x90 mm has been performed, resulting in the same damage evolution. The high speed camera records the damage in reflected light (flash-light and camera at the same side of the tile) and a 7.62 APM2 bullet hits the tile normal with 660 m/s. For comparison also a 19 mm thick float glass plate has been used to record its damage evolution upon bullet impact. Because glass is not hard enough to generate a dwell phase on impact by an AP round ($R_t < P$), here a 7.62 mild steel core bullet was used at 700 m/s impact velocity. This prevents the core to penetrate the glass directly upon impact as it will deform (rather than erode) on the strike-face. Although there are many differences between the damage evolution in glass and Spinel, there are similarities as well. Both show internal damage already in the first microsecond after impact. In Spinel almost half the tile thickness is involved in this early failure of material, which will be called impact damage in the rest of this work. The second part of the Spinel tile experiences not only dynamic loading but also tensile stress (due to tile bending) and at 3 microseconds individual cracks have crossed over to the rear of the tile already in a conical area below the impact zone. In the next few microseconds the damage area grows, expanding

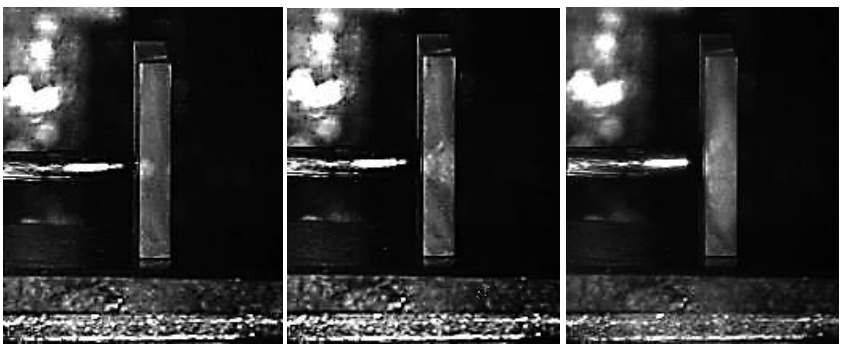

t = 1 µs t = 3 µs t = 6 µs

Figure 10. Damage evolution in 7 mm thick Spinel impacted with 7.62 APM2 at 660 m/s

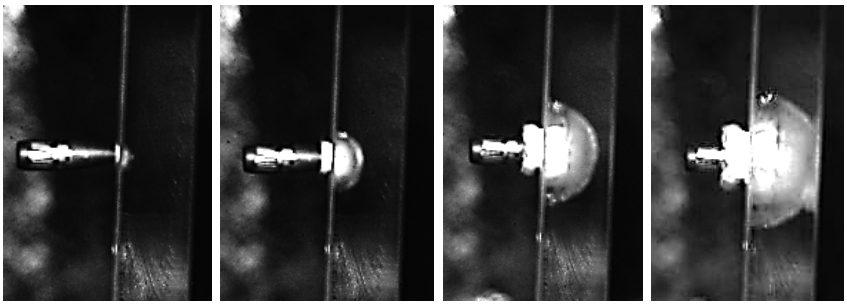

t = 1 µs t = 3 µs t = 8 µs t = 11 µs

Figure 11. Damage evolution in 19 mm thick float glass impacted with 7.62 MSC at 700 m/s

the conical damage area and the crack density seems to increase. First out-of-plane displacement occurs only at 14 microseconds.

In the float glass sample damage seems to occur in two regions that both radially expand from the impact site. The outer radius seems to be formed by individual cracks, while the inner region seems to consist of fully comminuted material as it reflects as a very bright zone. The individual cracks run faster (at about 1.9 km/s) than the comminution front and the first out-of-plane movement of glass fragments only occurs at 19 microseconds, suggesting an average comminution front velocity of 1.0 km/s. Its in-plane expansion is much easier to observe in the images than its through-the-thickness expansion. This is probably due to the blurring effect of the individual cracks running in front of it.

ENGINEERING MODEL

At TNO apart from the experimental work and computer simulations, we make use of energy-based engineering models to describe projectile-target interactions in a time-resolved fashion [18, 19]. Such models take only the main energy dissipating mechanism(s) into account and only use physical parameters and geometry of the projectile and target. The qualitative phenomena that are shown in figure 1 are well known and in principle easy to describe in an engineering model. The only problem that prevented us from making such engineering model for ceramics earlier was the unknown moment of the transition from dwell to out-of-plane flow of the ceramic, hence the duration of the dwell phase. In this work, the duration of the dwell time was found to have a linear dependency with the areal density of the target (both for bare ceramics and ceramics with backing layer). As long as the ceramic strike-face has a hardness (compressive strength) higher than the dynamic loading of the projectile it will be able to stop the nose of the projectile (at least temporarily). The duration of this dwell phase, in which the projectile nose is eroded, is mainly defined by the areal density of the target. It does not matter if the areal density is provided by a bare tile only, or by a thinner tile together with a backing layer. So, the dwell time could rather well be estimated using: $t_{Dwell} = AD * C$, with C a constant equal to the slope [dimension µs m^2/kg] in dwell versus areal density plots.

However, the laminated tiles (e.g. 2x 3.5 mm thick SiC or Si_3N_4) do not perform as well as a single tile with the same total thickness and areal density. And equally thick SiC tiles outperform Si_3N_4 tiles, although both have the same density (hence areal density). B_4C outperforms SiC, and SiC is considered a better armor ceramic than Alumina. But at equal tile thickness their areal densities would suggest an opposite ranking. Therefore, the duration of the dwell phase should be calculated taking also material specific parameters into account such as

impact damage and failure propagation time inside the bulk of a tile material. Note that such material specific parameters are not easily compared with static material properties, as they are more related to the failure dynamics of the material rather than its properties in the intact state.

The plots for dwell versus AD (or tile thickness) showed an off-set with respect to the origin, indicating that very thin tiles will not be able to induce a dwell time upon impact, due to impact damage. Impact damage has also been observed in dynamic fracture visualization experiments using glass and especially Spinel (see figure 11 and 10, respectively).

Therefore, in our engineering model the ceramic tile thickness t is converted into an effective thickness (t-x) due to immediate and/or erosion damage at the strike-face during the impact and dwell-phase. For ceramic tiles impacted by 7.62 APM2 at 830 m/s a value of x= 2 mm was shown to lead to good results. The time to convert the effective tile thickness to a fully (through the thickness) damaged material is calculated by (t-x)/w, with w the effective damage front velocity. From this moment on mainly the inertia of the sample (expressed by its areal density) increases the dwell time with AD * C, with C approximated by the slope of the line in figure 5. Both the existence of a critical tile thickness and damage velocity has been described earlier [e.g. 23]. Hence the dwell phase only occurs if $R_t > P$, with dynamic loading P given by equation 2, and its duration is composed of two parts, see figure 12:

$$t_{Dwell} = (t-x)/w + AD * C \qquad (5)$$

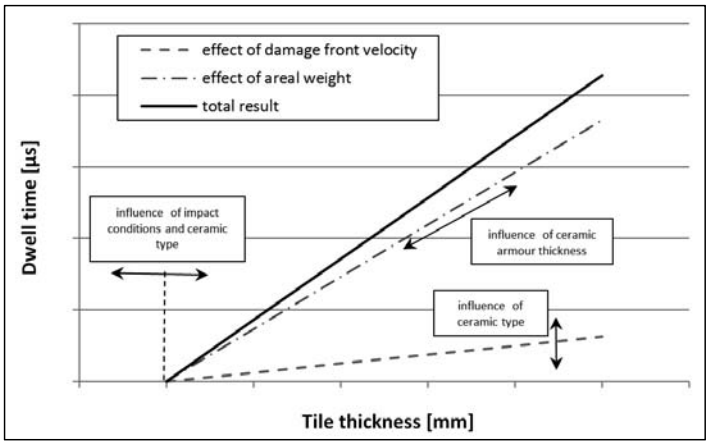

Figure 12. Representation of equation 5 with options for armor ceramic developments.

During the dwell-phase the impact pressure of the projectile is obtained from equation 2. By multiplication of this pressure with the current area of interaction (which increases during erosion of sharp nosed AP cores), the force on the residual mass of the core can be calculated for each time-step. Using $F=m_{c,i} * a_{c,i}$ the deceleration of the core can be obtained, providing the velocity drop of the core as a function of time. At the end of the dwell-phase ($t= t_{Dwell}$) the core has a certain mass and velocity. From this moment on its residual mass is constant (as erosion has stopped when U>0) and the residual velocity of the core is obtained using conservation of kinetic energy. The mass of the fragments in the truncated ceramic cone that is pushed out by the residual core is obtained using its volume and density of the ceramic. The dimensions of the truncated cone are obtained using the effective tile thickness, the radius of the projectile and a

cone angle of 40°. This average cone angle was obtained from the energy method on bare tiles of Alumina and SiC using the initial diameter of the fragment cloud [12], see the right-most image in figure 1. Using this calculation route the residual mass and velocity of an AP core can be calculated for a range of bare ceramics, layered ceramics, biceramics, and impact velocities.

However, for ceramic based armor the effect of energy absorption by the backing material has not yet been accounted for. The residual velocity of the core can be much lower if sufficient time and volume of backing material are involved in the interaction following the dwell phase. Therefore, for ceramic based armor the residual velocity of the core as obtained using our engineering model for ceramic targets can be considered as an upper bound. Table 2 shows a comparison of dwell times as obtained from the energy method and calculated using equation 5 for several bare ceramics, tile thicknesses, biceramics, as well as ceramic based armor using a wide range of backing materials. The values are generally in good agreement, especially considering the simplicity of the calculation method and wide variation of target types. Both the biceramic samples and the ceramic based armor samples have been treated taking the first layer as ceramic strike-face in which impact damage and a damage front propagates, while for the second component only its areal density was used. Notice the 46 mm Al backing, representing a semi-infinite DoP test sample, generates an extremely long dwell time that is not representative for a realistic ceramic based armor system.

Table 2: Comparison in duration of dwell time as obtained with the energy test method (experiments) and calculation using equation 5 for 7.62 APM2 impacting bare tiles, biceramic and ceramic based armor targets at 830 m/s.

Bare tile samples	Dwell time Energy M [μs]	Dwell time Calculated [μs]	Ceramic based armor	Dwell time Energy M [μs]	Dwell time Calculated [μs]
Alumina 1	5,0	5,2	Alumina + 10mm Dyneema HB26	8,5	9,0
Alumina 2	8,9	8,7	Alumina + 5mm Dyneema HB26	12,5	10,5
Alumina 3	13,8	13,9	Alumina + 3mm Steel 52	10,6	14,0
Alumina 4	17,4	17,4	Alumina + 3,3mm ARMOX 500	14,0	14,9
Alumina 5	22,1	22,6	Hexalloy SiC + 2 mm 6082 Alu	10,6	9,7
Spinel	7,5	8,0	Hexalloy SiC + 2*2 mm 6082 Alu	12,6	11,7
Hexalloy SiC	8,2	7,7	Hexalloy SiC + 3*2 mm 6082 Alu	12,6	13,7
SiC F 1	14,3	13,6	Hexalloy SiC + 4*2 mm 6082 Alu	15,7	15,8
SiC F 2	17,8	17,0	Hexalloy SiC + 46 mm 2024 Alu	-	54,2

Biceramic samples	Dwell time Energy M [μs]	Dwell time Calculated [μs]
SiC/Corbit98	9,8	7,5
2x Corbit98	6,7	8,0
Corbit98 + Alocor100	16,3	14,5
SiC + ZrO2	17,8	21,4
SiC + ZrO2	20,4	25,3

CONCLUSION

The energy test-method has been applied to a wide range of ceramic materials, including SiC, Alumina, Si_3N_4, ZrO_2, biceramics and step-graded ceramics as well as a range of ceramic tiles with various backing materials. This method not only allows to determine a global ballistic efficiency factor, but also provides an estimated duration of the dwell-phase for each sample.

A linear relation was obtained between the dwell time and areal density of bare ceramic samples, as well as for ceramic based armor (ceramic with backing layer). The same linear relation as was found for the dwell time was also obtained using high speed shadowgraphy of normally impacted translucent Alumina samples. Here the radial expansion of a darkened (hence damaged) zone was recorded at high temporal resolution. The moment the expansion of this zone stopped is thought to be caused by the arrival of damage (comminution) at the rear of the tile allowing the residual projectile to axially plug out a conical volume of fragments. This axial movement marks the end of the dwell-phase of the projectile-target interaction.

There was an off-set in the t_{Dwell}-AD relation as the line does not go through the origin. This indicates that there is a minimal tile thickness required for a ceramic (with a hardness above that of the threat) to generate a significant dwell-phase upon impact of a projectile.

Also high speed imaging was applied to transparent samples of float glass and Spinel tiles. In a side-view the damage progression inside these transparent samples could be recorded showing impact damage to occur in the first microsecond in both types of materials. The occurrence of impact damage alone, or reduced erosion resistance induced by it, may explain the apparent minimal tile thickness which seems to be required for the dwell phase to occur. Although individual cracks run very fast away from the impact area, first out-of-plane deformation of the targets was only observed after the arrival of a damage front at the rear of the strike face. Behind this damage front the material seems to be comminuted.

The estimated duration of the dwell-phase of bare ceramics, biceramic samples, as well as ceramic samples with (a wide range of) backing materials have been experimentally determined using the energy-method. A simple equation has been suggested that allows this duration of the dwell-phase to be calculated. The quantification of the duration of this most important phase of the projectile-target interaction of ceramic based armor allows an engineering model to be used in which both the residual mass and velocity of a (AP) projectile core can be calculated. During the dwell-phase the projectile has an erosion velocity V. From the dynamic loading the resulting force on the projectile nose is obtained, which allows the reduction of V as a function of time to be calculated. After t_{Dwell} the residual mass of the projectile is fixed (as erosion has stopped), while the residual velocity is obtained using conservation of energy due to acceleration of a truncated cone of ceramic fragments (and a backing material).

The impact/erosion damage depth (x) at the strike face and velocity of the damage front (W) through the strike-face material should be experimentally obtained, as they do not seem to have a unique relation with the mechanical properties of the ceramic. The energy test-method is a convenient way to determine these relevant values for all ceramic based armor and armor ceramic tiles. For transparent and translucent ceramic targets the same data can also be obtained using high speed optical techniques.

ACKNOWLEDGEMENTS

Prof. Jef Vleugels and Dr. Shuigen Huang of Catholic University of Leuven, Belgium are acknowledged for the manufacturing of step-graded ceramic samples by Spark Plasma Sintering (SPS) and measuring of their mechanical properties.

REFERENCES

[1] A. Krell, et al., Separation and Hierarchic Order of Key Influences on the Ballistic Strength of Opaque and Transparent Ceramic Armor, *27th International Symposium on Ballistics*, 1053-1064 (2013)
[2] P. Hazell, et al., The design of mosaic armour: The influence of tile size on ballistic performance, *Materials and Design*, **29,** 1497–1503 (2008)
[3] S. LaSalvia, et al., Beyond hardness: Ceramics and ceramic-based composites for protection, *JOM* **62** (1) 1543-1551 (2010)
[4] S. Sarva et al., The effect of membrane restraint on the ballistic performance of armor grade ceramic tiles, *Int. J. Impact Engineering*, **34,** 277-302 (2007)
[5] P.R.S. Reddy, et al., Influence of polymer restraint on ballistic performance of alumina ceramic tiles, *Defence Science Journal*, **58** (2), 264-274 (2008)
[6] P. Hazell, *Advances in Applied Ceramics*, vol.109 (8), pp. 504-510
[7] A. Tate, A theory for the deceleration of long rods after impact, *J. Mech. Phys. Solids*, 15, pp. 387-99 (1967)
[8] D. Shockey et al., The damage mechanism route to better armor materials, *Int. J. Impact. Engng.* 7 (5), 566-573
[9] P.G. Kanrandikar et al., A review of ceramics for armor applications, *Ceram Eng. Sci. Proc.* 29 (6), 45
[10] E.J. Haney and G. Subhash, Damage mechanisms perspective on superior ballistic performance of Spinel over Sapphire, *Experimental Mechanics* (2013) 53, p. 31-46
[11] private communication with Ardi Dortmans (TNO)
[12] E. Carton, Alternative test method for armor ceramics and ceramic-based armor, *38th ICACC,* Daytona Beach, Fl (2014)
[13] E. Carton et al., Particle and fragment size distribution of impacted ceramic tiles,*28th International Symposium on Ballistics*, Atlanta, USA (2014) 1254
[14] E. Medvedovski, Ballistic performance of armour ceramics: Influence of design and structure. Part 1, *Ceramics International* 36 (2010) 2103–2115
[15] D. Shockey et al., The damage mechanism route to better armor materials, *Int. J. Impact. Engng.* 7 (5) 566-573
[16] P.G. Kanrandikar et al., A review of ceramics for armor applications, *Ceram Eng. Sci. Proc.* 29 (6) 45
[17] E.J. Haney and G. Subhash, Damage mechanisms perspective on superior ballistic performance of Spinel over Sapphire, *Experimental Mechanics* 53 (2013) 31-46
[18] E.P. Carton and G. Roebroeks, Time resolved engineering metal penetration models, *27th International Symposium on Ballistics*, Miami, USA (2011) 1280
[19] G. Roebroeks and E.P. Carton, Engineering model for impact of blunt projectiles on metallic sheets, *28th International Symposium on Ballistics,* Atlanta, USA (2014) 1276
[20] H. Horii and S. Nemat-Nasser, *Phil. Trans. R. Soc. London A* (1986) 337
[21] J. LaSalvia et al. Microstructural and micromechanical aspects of ceramic/long-rod projectile interactions: dwell/penetration transitions, *Fundamental Issues and Applications of Shock-wave and High-Strain-Rate Phenomena* (2001) 437 – 446
[22] J. LaSalvia et al., A physically-based model for the effect of microstructure and mechanical properties on ballistic performance, *26th Annual Conference on Composites, Advanced Ceramics, Materials, and Structures: A: Ceramic Engineering and Science Proceedings*, Volume 23, Issue 3
[23] N.K. Bourne, Z. Rosenberg and J.E. Field, Failure zones in polycrystalline aluminas, *Proc. R. Soc. Lond. A,* 455 (1999) 1267-1274